

MIT Open Access Articles

Ferromagnetic transition in a one-dimensional spin-orbit-coupled metal and its mapping to a critical point in smectic liquid crystals

The MIT Faculty has made this article openly available. **Please share** how this access benefits you. Your story matters.

Citation: Kozii, Vladyslav et al. "Ferromagnetic transition in a one-dimensional spin-orbit-coupled metal and its mapping to a critical point in smectic liquid crystals." *Physical Review B* 96, 9 (September 2017): 094419 © 2017 American Physical Society

As Published: <http://dx.doi.org/10.1103/PhysRevB.96.094419>

Publisher: American Physical Society

Persistent URL: <http://hdl.handle.net/1721.1/114526>

Version: Final published version: final published article, as it appeared in a journal, conference proceedings, or other formally published context

Terms of Use: Article is made available in accordance with the publisher's policy and may be subject to US copyright law. Please refer to the publisher's site for terms of use.



Ferromagnetic transition in a one-dimensional spin-orbit-coupled metal and its mapping to a critical point in smectic liquid crystals

Vladyslav Kozii,¹ Jonathan Ruhman,¹ Liang Fu,¹ and Leo Radzihovsky^{2,3}

¹*Department of Physics, Massachusetts Institute of Technology, Cambridge, Massachusetts 02139, USA*

²*Department of Physics, Center for Theory of Quantum Matter, and JILA, University of Colorado, Boulder, Colorado 80309, USA*

³*Kavli Institute for Theoretical Physics, University of California, Santa Barbara, California 93106, USA*

(Received 1 June 2017; revised manuscript received 26 August 2017; published 18 September 2017)

We study the quantum phase transition between a paramagnetic and ferromagnetic metal in the presence of Rashba spin-orbit coupling in one dimension. Using bosonization, we analyze the transition by means of renormalization group, controlled by an ε expansion around the upper critical dimension of two. We show that the presence of Rashba spin-orbit coupling allows for a new nonlinear term in the bosonized action, which generically leads to a fluctuation driven first-order transition. We further demonstrate that the Euclidean action of this system maps onto a classical smectic-A–C phase transition in a magnetic field in two dimensions. We show that the smectic transition is second order and is controlled by a new critical point.

DOI: [10.1103/PhysRevB.96.094419](https://doi.org/10.1103/PhysRevB.96.094419)

I. INTRODUCTION

A. Background and motivation

Quantum phase transitions continue to be one of the central topics in condensed matter physics. The problem is especially challenging in systems of itinerant electrons. The first attempts to describe the critical behavior of interacting itinerant electrons were made by Hertz [1] and Millis [2] in the context of the ferromagnetic (FM) and antiferromagnetic phase transitions. They constructed an effective Ginzburg-Landau theory by integrating out fermionic degrees of freedom. However, nonanalyticities generated by integrating out gapless electrons call into question the validity of this uncontrolled approach. To avoid these dangerous singularities, the gapless fermions and the soft bosonic order parameter must be treated on equal footing [3–6]. However, the theory still exhibits a divergent perturbation theory associated with gapless Fermi surface degrees of freedom, whose control remains an open problem [7–14].

In contrast, in one dimension, bosonization of the electronic quasiparticles significantly simplifies the problem, making it tractable. This approach, combined with a renormalization group (RG) analysis, was successfully applied by Yang [15] to analyze the quantum transition from paramagnetic (PM) phase to an Ising itinerant ferromagnet in a one-dimensional conductor. The resulting strongly-interacting critical point is distinct from the Luttinger liquid and Ising critical points, and in one-loop approximation is characterized by the dynamic critical exponent $z = 2$. Later, similar results for a one-dimensional Heisenberg ferromagnet were obtained in Ref. [16].

The possibility of a ferromagnetic ground state seemingly contradicts the Lieb and Mattis theorem [17], which states that an unmagnetized state always has lower energy for certain classes of systems. This theorem, however, does not take into account spin-orbit coupling, which will play an important role in our study. Furthermore, it was shown that the inclusion of further neighbor hopping terms in the lattice models [18], as well as a spin-dependent interaction, can also stabilize a ferromagnetic ground state. Finally, numerical results obtained in Ref. [18] suggest an existence of a ferromagnetic transition

in one-dimensional systems. Taken together, these arguments demonstrate that Lieb-Mattis theorem is not applicable in the most general system, studied in this work, implying that the problem of a one-dimensional ferromagnetic transition is well-defined and meaningful.

The model of a ferromagnetic transition studied in Ref. [15] does not take into account generically present spin-orbit coupling and relies on the presence of inversion symmetry. In systems that lack inversion symmetry, however, the presence of Rashba spin-orbit coupling leads to interesting physical consequences. It naturally reduces the $SU(2)$ spin rotation symmetry to a $U(1)$ symmetry associated with the total S_z conservation, and, as a result, the ferromagnetic transition becomes of the Ising type. This situation is very common in realistic experimental setups with spin-orbit-coupled wires, where Rashba coupling appears, e.g., due to the internal crystal structure or due to external sources, such as the substrate, gates, etc.

Motivated by this observation, in this paper we consider the most general case of the ferromagnetic transition in spin-orbit-coupled one-dimensional metals, without assuming any other symmetry except time reversal. We study it via an RG analysis controlled by an ε expansion. We show that, in the absence of inversion symmetry, nonlinear coupling between spin current and magnetization enhances quantum fluctuations, which *generically* drive the itinerant ferromagnetic transition first order, akin to a compressible Ising model [19]. As a special case, when inversion symmetry is present, we recover the continuous transition found in Ref. [15].

We further show that the bosonic Euclidean (imaginary time) $D = 1 + 1$ dimensional action of an itinerant magnetic wire maps onto a field theory describing a classical two-dimensional ($D = 2$) smectic-A to smectic-C phase transition in a magnetic field, studied at upper critical dimension, $D = 3$, by Grinstein and Pelcovits in their seminal work [20]. They showed that, at $D = 3$, the transition is controlled by the Gaussian fixed point, and correlation functions exhibit mean-field-like behavior with logarithmical corrections to scaling. We reproduce their results in $D = 3$. In addition, we analyze the system below the upper critical dimension, $D < 3$,

where the Gaussian fixed point becomes unstable. We find a new strongly-interacting stable fixed point which controls the second-order transition.

For bare couplings satisfying a special relation, which corresponds to a rotationally invariant smectic, the model we consider reduces to that of anomalous elasticity [21] of a two-dimensional smectic-A liquid crystal. This problem was solved exactly by Golubovic and Wang [22,23] through mapping onto the 1 + 1 dimensional Kardar-Parisi-Zhang equation [24]. Thus, our theory reproduces results known in literature as special limiting cases.

The remainder of the paper is organized as follows. We conclude the Introduction with a summary of our results. In Sec. II, we present a microscopic model for the Ising transition in an itinerant ferromagnet, including the effect of Rashba spin-orbit coupling. Utilizing bosonization we derive an effective low-energy field theory for this transition. In Sec. III, by generalizing the field theory to $D = d + 1$ dimensions, we analyze this transition using renormalization group methods, controlled by an $\varepsilon = 3 - D$ expansion. In Sec. IV, we apply these results to a mathematically related classical problem of a smectic-A to smectic-C transition in a magnetic field and obtain a nontrivial critical point in two dimensions. We summarize our results and conclude in Sec. V.

B. Results

Before presenting technical details we briefly summarize our findings. We develop a field-theoretic model for a quantum phase transition to an itinerant ferromagnet in the presence of Rashba spin-orbit coupling. In contrast to a special case of inversion-symmetric system [15], we show that generically it exhibits an additional nonlinearity with a coupling $g_1 > 0$, which is relevant for $D = d + 1 < 3$, and thus the transition is governed by a qualitatively distinct behavior [see Sec. III and Eq. (26) for the definition of g_1].

Utilizing a one-loop RG method, controlled by an $\varepsilon = 3 - D$ expansion, we show that, akin to a compressible Ising model [19], the inversion-symmetry breaking nonlinearity $g_1 > 0$, together with strong quantum fluctuations, generically drive the itinerant ferromagnetic transition first order. While our analysis relies on an analytical continuation of a 1d bosonized model to high dimensions, we conjecture that this fluctuations-driven first-order transition is a qualitative feature that extends to two- and three-dimensional ferromagnets without inversion symmetry [14,25].

The imaginary time (Euclidean) action of the model characterizes the classical Sm-A to Sm-C liquid crystal transition in a magnetic field, extending seminal work of Grinstein and Pelcovits away from the marginal dimension of $D = 3$ down to $D = 2$. Specifically we find that for $g_1 < 0$, within the one-loop $\varepsilon = 3 - D$ expansion ($\varepsilon = 1$ for the physical case), the new critical point that controls the transition is characterized by

$$\begin{aligned} z &= 2 - \frac{3\varepsilon}{37}, & \nu &= \frac{1}{2} + \frac{9\varepsilon}{74}, \\ \gamma &= 1 + \frac{\varepsilon}{74}, & \beta &= \frac{1}{2} - \frac{5\varepsilon}{37}, \end{aligned} \quad (1)$$

where z , ν , γ , and β are dynamical, correlation length, susceptibility, and order parameter critical exponents, respectively. Within the global phase diagram of the Euclidean field theory the continuous transition criticality for $g_1 < 0$ is separated from the first-order fluctuation-driven transition for $g_1 > 0$ by the $g_1 = 0$ inversion-symmetric tricritical point [15].

II. MICROSCOPIC MODEL FOR 1D ITINERANT FERROMAGNETIC TRANSITION

We begin with a generic microscopic model of a one-dimensional metal with Rashba spin-orbit coupling, characterized by an electronic Hamiltonian (choosing units such that $\hbar = k_B = 1$)

$$H = H_0 + H_{\text{so}} + H_{\text{int}}, \quad (2)$$

where

$$H_0 = \sum_s \int dx \psi_s^\dagger(x) [\varepsilon(-i\partial/\partial x) - \varepsilon_F] \psi_s(x) \quad (3)$$

is a single-particle band Hamiltonian, characterized by a dispersion $\varepsilon(-i\partial/\partial x)$, Fermi level ε_F , and $s = \uparrow, \downarrow$ labels electron spin projection. H_{int} accounts for forward- and backscattering processes.

The second contribution,

$$H_{\text{so}} = \alpha_R \sum_{s,s'} \int dx \psi_s^\dagger(x) \sigma_{ss'}^z (-i\partial/\partial x) \psi_{s'}(x), \quad (4)$$

is the Rashba spin-orbit coupling, which is odd under inversion. As mentioned above, we expect this term to apply to many realistic experimental setups, including semiconducting nanowires with strong spin-orbit coupling [26–28] and non-centrosymmetric quasi-one-dimensional materials.

To study the ferromagnetic transition, we now derive the corresponding low-energy Hamiltonian. Focusing on the vicinity of the Fermi points at momenta $\pm k_F$, we expand the electron field operators

$$\psi_s(x) \approx \psi_{sR}(x) e^{ik_F x} + \psi_{sL}(x) e^{-ik_F x} \quad (5)$$

in terms of left ($r = L$) and right ($r = R$) moving fields $\psi_{sr}(x)$ varying slowly on the scale of Fermi wavelength, $\lambda \sim 1/k_F$, and satisfying usual anticommutation relations $\{\psi_{sr}(x), \psi_{s'r'}(x')\} = \delta_{ss'} \delta_{rr'} \delta(x - x')$. In terms of the ‘slow’ fields $\psi_{sR(L)}$, Rashba spin-orbit coupling reduces to

$$H_{\text{so}} = \alpha_R k_F \sum_{r,s} \int dx r s n_{sr}(x) = \alpha_R k_F \int dx J, \quad (6)$$

where we defined spin density $n_{sr}(x) = \psi_{sr}^\dagger(x) \psi_{sr}(x)$ and spin current density J . Both $s = \uparrow, \downarrow$ and $r = R, L$ correspond to $+1, -1$, respectively.

In terms of the slow chiral fields the band Hamiltonian in Eq. (2) reduces to $H_0 = \sum_n H_{(n)}$, with

$$H_{(n)} = \frac{\partial_k^{(n)} \varepsilon(k)}{n!} \Big|_{k=k_F} \sum_{r,s} \int dx \psi_{sr}^\dagger(x) (-ir\partial_x)^n \psi_{sr}(x). \quad (7)$$

Terms with $n \geq 2$ originate from the curvature of the band dispersion around Fermi points $\pm k_F$ and are often neglected.

However, they are crucial here to properly describe the itinerant FM transition.

Equation (2) with short-range interaction, $H_{\text{int}} = U \int dx n_{\uparrow}(x)n_{\downarrow}(x)$, and without spin-orbit coupling, $\alpha_R = 0$, is precisely a starting point for Hertz-Millis analysis in higher dimensions. It is studied by introducing a Hubbard-Stratonovich magnetization order parameter to decouple the interaction and by integrating out electrons to obtain the nonlocal Landau action for the magnetization. Such an analysis, however, has been shown to be oversimplified, since it does not take into account massless fermionic modes carefully, neglecting important nonanalyticities appearing after integrating out electrons, and thus unlikely to describe the true critical behavior.

To avoid the aforementioned difficulties with the Hertz-Millis approach, here we will utilize the power of one-dimensional Abelian bosonization to derive an effective bosonic theory that we will then study by conventional Wilsonian RG [29]. Following standard bosonization procedure [30], we write electronic operators in terms of bosonic phase fields:

$$\psi_{sr} = \frac{F_s}{\sqrt{2\pi a}} e^{irk_F x} e^{\frac{i}{\sqrt{2}}(\phi_{\rho} + s\phi_{\sigma} - r\theta_{\rho} - rs\theta_{\sigma})}, \quad (8)$$

where F_s are Klein factors, a is a short-range cutoff, and fields ϕ and θ obey commutation relations

$$[\partial_x \phi_{\alpha}(x), \theta_{\alpha'}(x')] = -i\pi \delta_{\alpha\alpha'} \delta(x - x'). \quad (9)$$

Here $\alpha, \alpha' = \rho, \sigma$ label charge and spin degrees of freedom, $\rho(x) = -(\sqrt{2}/\pi)\partial_x \theta_{\rho}$ and $S_z(x) = -(\sqrt{2}/\pi)\partial_x \theta_{\sigma}$ are charge and spin densities, and $J_c(x) = (\sqrt{2}/\pi)\partial_x \phi_{\rho}$ and $J(x) = (\sqrt{2}/\pi)\partial_x \phi_{\sigma}$ are charge and spin currents, respectively.

At length scales much longer than the Fermi wavelength, $1/k_F$, and at low energy, the effective bosonized Hamiltonian takes the standard form

$$H = \sum_{\alpha=\rho,\sigma} \frac{u_{\alpha}}{2\pi} \int dx \{ \mathcal{K}_{\alpha} (\partial_x \phi_{\alpha})^2 + \mathcal{K}_{\alpha}^{-1} (\partial_x \theta_{\alpha})^2 \} + \frac{\gamma}{2\pi^2 a^2} \int dx \cos \sqrt{8}\theta_{\sigma} + H_{\text{nl}} + H_{\text{so}}. \quad (10)$$

The parameters $u_{\sigma,\rho}$ correspond to the velocity of spin and charge excitations, respectively, while $\mathcal{K}_{\sigma,\rho}$ are the Luttinger parameters that characterize the sign and strength of forward scattering interaction [30].

The relevance of the cosine term is controlled by the spin Luttinger parameter K_{σ} . When $K_{\sigma} < 1$, the cosine pins the spin-density variable θ_{σ} , leading to the formation of a spin gap [31]. On the other hand, when $K_{\sigma} > 1$, it is irrelevant and flows to 0 under RG. In the latter case, its only effect is to renormalize the Luttinger parameters at low energies and thus can be neglected.

As in a conventional Landau theory [32,33], classically, the transition to the ferromagnetic state takes place when the coefficient in front of $S_z^2 \sim (\partial_x \theta_{\sigma})^2$ is tuned to be zero. Close to the transition the coefficient at S_z^2 is small, corresponding to $\mathcal{K}_{\sigma} \rightarrow \infty$. Consequently, the cosine term in Eq. (10) is irrelevant and thus neglected hereafter [34].

In contrast, there are higher-order terms that are typically neglected near the LL fixed point, but, as we demonstrate below, become important at the ferromagnetic transition.

These terms are taken into account in H_{nl} ; they describe nonlinear couplings between spin density and spin current, as well as between spin and charge sectors, that arise, for example, due to the finite curvature of the electronic dispersion. Since the coefficient of S_z^2 term vanishes at the transition, it is necessary to keep these higher order in S_z terms in order to stabilize the theory. Furthermore, as we will show, they are relevant in the RG sense, and thus play a qualitatively important role at low energies.

We further take advantage of spin-charge separation at the quadratic order and completely neglect the charge sector, focusing only on the spin sector controlling the transition to a state with finite magnetization S_z [35]. Then, the higher-order terms that are necessary for the stability of the theory are given by

$$H_{(3)} = \int dx \{ \beta_4 [S_z^4 + 6S_z^2 J^2] + \beta_2 (\partial_x S_z)^2 \} = \beta_0 \int dx \{ [(\partial_x \theta_{\sigma})^4 + 6(\partial_x \phi_{\sigma})^2 (\partial_x \theta_{\sigma})^2] + 2(\partial_x^2 \theta_{\sigma})^2 \}, \quad (11)$$

where $\beta_0 = 4\beta_4/\pi^4 = \beta_2/\pi^2 = (1/48\pi)(\partial_k^3 \epsilon_k)_{k=k_F}$, and we neglected terms that are less relevant. To derive Eq. (11), we used a standard point-splitting technique for normally-ordered operators, which allows, in principle, to calculate all higher-order terms. The details of such derivation can be found, for instance, in Ref. [36], and we thus do not present it here. The terms in Eq. (11) describe the coupling between magnetization and spin current, thus contributing to H_{nl} in Eq. (10). We note that the sign of β_0 depends on the third derivative of the dispersion near the Fermi energy. Here we focus on the more interesting case when this coefficient is positive, since the opposite case of $\beta_0 < 0$ leads to a first-order transition, already at the Landau mean-field theory level.

We now examine the inversion-breaking contribution (6), that is linear in spin current $J = (\sqrt{2}/\pi)\partial_x \phi_{\sigma}$, and as expected induces a finite spin current in the ground state. It can thus be absorbed into (10) by shifting the spin current according to $\tilde{J} = J + 2\alpha_R k_F / \pi u_{\sigma} \mathcal{K}_{\sigma}$, with \tilde{J} describing fluctuations about the nonzero ground state spin current.

Focusing on the spin sector [35], and putting above contributions together, we obtain a low-energy Hamiltonian for the one-dimensional itinerant Ising ferromagnetic transition,

$$H = \int dx \{ \alpha_J \tilde{J}^2 + \alpha_S S_z^2 + \beta_2 (\partial_x S_z)^2 - \lambda_3 \tilde{J} S_z^2 + \beta_4 S_z^4 \}, \quad (12)$$

where $\lambda_3 = 6\pi\beta_2\alpha_R k_F / u_{\sigma} \mathcal{K}_{\sigma}$, $\alpha_J = u_{\sigma} \mathcal{K}_{\sigma} \pi / 4$, and $\alpha_S = (u_{\sigma} \pi / 4 \mathcal{K}_{\sigma}) + (6\alpha_R^2 k_F^2 \pi^2 / u_{\sigma} \mathcal{K}_{\sigma})$, and operators obey a commutation relation

$$[\tilde{J}(x), S_z(x')] = -i \frac{2}{\pi} \partial_x \delta(x - x'). \quad (13)$$

The coefficient λ_3 is proportional to the spin current in the system and thus is a direct manifestation of inversion breaking. This term is absent in Ref. [15], where the inversion-symmetric case has been considered.

We note that the above quantum Hamiltonian takes the form of a standard Landau theory but supplemented with a canonical

commutation relation (13), with the spin current $\tilde{J} \sim \partial_x \tilde{\phi}_\sigma$ playing the role of the canonically conjugate momentum density for the spin phase field θ_σ . The model (12) has been derived for a one-dimensional metal with Rashba spin-orbit coupling. Note, however, that this model also applies to magnetic spin chains with Dzyaloshinskii-Moriya interaction.

III. BREAKDOWN OF QUANTUM CRITICALITY AT THE FM TRANSITION

A. Effective field theory

To study the critical properties of the resulting model, we focus on the partition function, $Z = \text{Tr}[\exp(-\beta H)]$, and express it through the imaginary time functional integral over commuting conjugate fields $\phi_\sigma, \theta_\sigma$ in a standard way

$$Z = \int D\theta_\sigma D\Pi \exp \left[- \int_0^\beta d\tau \int dx (H - i\Pi \partial_\tau \theta_\sigma) \right], \quad (14)$$

where $\beta = 1/T$ is the inverse temperature, and Hamiltonian H depends on the canonically conjugate fields $\theta_\sigma(x)$ and $\Pi(x) = \partial_x \tilde{\phi}_\sigma(x)/\pi$. Integrating over the momentum field $\partial_x \tilde{\phi}_\sigma$, we obtain $Z = \int D\theta e^{-S}$, where the imaginary-time action for a quantum itinerant PM-FM transition is given by

$$S = \int d^d x d\tau \left\{ \frac{r}{2} (\nabla\theta)^2 + \frac{K}{2} (\nabla^2\theta)^2 + \frac{B}{2} (\partial_\tau\theta)^2 - \frac{iB_3}{2} (\partial_\tau\theta)(\nabla\theta)^2 + \frac{B_4}{8} [(\nabla\theta)^2]^2 \right\}. \quad (15)$$

Above we dropped the index σ for brevity, and generalized the field theory to d spatial dimensions, as it will be necessary for the ε -expansion analysis. Hereafter, we use $D = d + 1$ for the total number of space-time dimensions, while d stands for a number of spatial dimensions. We stress that the physically meaningful case corresponds to $d = 1$ (quantum wire), while the extension of action (15) to dimensions outside of 1d is used here as a mathematical tool only, in the spirit of ε expansion, to treat and control strong critical quantum fluctuations.

In principle, all coefficients in the action (15) can be expressed through the parameters entering the microscopic Hamiltonian, Eq. (12). However, we prefer not to specify them explicitly, treating them as phenomenological parameters, thereby emphasizing that there is a number of microscopic contributions to this action, beyond what we considered in the previous section. The action (15) captures all universal properties of the itinerant PM-FM transition in 1d, and, although in principle is derivable from the microscopic model, can be written based purely on symmetry arguments. We only require that $K, B, B_4 > 0$; otherwise, higher-order terms will be needed to stabilize the theory, and the transition will be first order even at the mean-field level.

As mentioned in the previous section, the first term in the action (15), $r(\nabla\theta)^2/2$, tunes the model to the FM transition, at mean-field level $r < 0$ ($r > 0$) corresponding to the ordered FM phase (disordered PM phase). The third term in Eq. (15) describes fluctuations along imaginary time, capturing the quantum nature of the transition. Clearly, at the critical point ($r = 0$ in mean-field theory), higher-order terms in spatial gradient (K) and in the magnetization ($B_{3,4}$) are required to

ensure the stability of the system to large and nonuniform magnetization. As we showed above, the term proportional to B_3 arises from the coupling between magnetization and spin current, i.e., proportional to λ_3 in the Hamiltonian (12). B_3 breaks inversion symmetry and will be of special significance in our analysis.

We note that there is a certain similarity between our model (15) and (12) and the compressible Ising model [19]. In the latter case, the system can gain energy by adjusting compressible lattice to the local spin configuration. As a result, sufficiently close to the putative critical point it is generically unstable to a discontinuous development of a spontaneous magnetization (accompanied by a lattice distortion), thereby undergoing a first-order transition. We anticipate and indeed find a similar mechanism in our model. Namely, we expect that an inversion-symmetry breaking that couples spin current and spin density, $iB_3(\partial_\tau\theta)(\partial_x\theta)^2$, will generically drive the FM transition first order associated with a discontinuous jump in the spin current and magnetization. There are, however, two important differences between these two models. First, unlike the compression modes of charge, the spin current is not a conserved quantity. Second, the spin current, which is represented by the term $i\partial_\tau\theta$, and the spin density, $\partial_x\theta$, are not independent fields. Thus, a detailed analysis is required to which we now turn.

B. Harmonic fluctuations

Away from the critical point, deep in the PM, $r > 0$ state, higher-order gradients and nonlinearities are unimportant. In this limit, the action (15) reverts to that of a conventional Luttinger liquid, described by a $1 + 1$ dimensional XY model, with well studied logarithmic phase correlations [30].

At the critical point, $r = 0$, within a harmonic approximation (neglecting nonlinearities) the action maps onto that of a well-studied $d + 1$ -dimensional smectic liquid crystal [37–39], with the imaginary time axis and spin phase $\theta(\mathbf{x}, \tau)$ corresponding to the smectic wave vector (layer normal) axis τ and the phonon $u(\mathbf{x}, \tau)$, respectively. At the critical point the fluctuations are qualitatively enhanced, characterized by $z = 2$ (rather than $z = 1$) dynamical exponent, with mean-squared fluctuations in the ground state ($T = 0$) given by

$$\langle \theta^2 \rangle_0 = \int_{L^{-1}}^{a^{-1}} \frac{d^d k d\omega}{(2\pi)^{d+1}} \frac{1}{B\omega^2 + Kk^4} \quad (16a)$$

$$\approx \begin{cases} \frac{1}{2(2-d)\sqrt{BK}} C_d L^{2-d}, & d < 2, \\ \frac{1}{4\pi\sqrt{BK}} \ln(L/a), & d = 2, \end{cases} \quad (16b)$$

where we defined a constant $C_d = S_d/(2\pi)^d = 2\pi^{d/2}/[(2\pi)^d \Gamma(d/2)]$, with S_d a surface area of a d -dimensional sphere ($S_1 = 2$, $S_2 = 2\pi$, $S_3 = 4\pi$, etc.), and introduced a spatial infrared (IR) cutoff by considering a system of finite spatial extent L and an ultraviolet (UV) cutoff a , set by the underlying lattice constant or a Fermi wavelength $\sim k_F^{-1}$. We note that for $d \leq 2$ and in particular for the case of physical interest, $d = 1$, harmonic quantum fluctuations diverge (stronger than a conventional Luttinger liquid) with system size, suggesting a qualitative importance of nonlinearities.

The corresponding connected harmonic correlation function

$$C(\mathbf{x}, \tau) = \langle [\theta(\mathbf{x}, \tau) - \theta(\mathbf{0}, 0)]^2 \rangle_0 \quad (17)$$

is also straightforwardly worked out. At the critical point in $2 + 1$ space-time dimensions, in the ground state ($T = 0$) it is given by the logarithmic Caillé form [39]

$$\begin{aligned} C^{3D}(\mathbf{x}, \tau) &= 2 \int \frac{d^2 k d\omega}{(2\pi)^3} \frac{1 - e^{i\mathbf{k}\cdot\mathbf{x} - i\omega\tau}}{Kk^4 + B\omega^2} \\ &= \frac{1}{2\pi\sqrt{KB}} \left[\ln\left(\frac{x}{a}\right) - \frac{1}{2} \text{Ei}\left(\frac{-x^2}{4\lambda|\tau|}\right) \right], \end{aligned} \quad (18a)$$

$$\approx \frac{1}{4\pi\sqrt{KB}} \begin{cases} \ln(x^2/a^2), & x \gg \sqrt{\lambda|\tau|}, \\ \ln(4\lambda|\tau|/a^2), & x \ll \sqrt{\lambda|\tau|}, \end{cases} \quad (18b)$$

where $\text{Ei}(x)$ is the exponential-integral function and $\lambda = \sqrt{K/B}$. As indicated in the last form, in the asymptotic limits of $x \gg \sqrt{\lambda\tau}$ and $x \ll \sqrt{\lambda\tau}$ this 3D correlation function reduces to logarithmic growth with x and τ , respectively.

In the case $D = 1 + 1$ of physical interest we instead have [40]

$$\begin{aligned} C^{2D}(x, \tau) &= \int \frac{dk d\omega}{(2\pi)^2} \frac{1 - e^{ikx - i\omega\tau}}{Kk^4 + B\omega^2} \\ &= \frac{1}{B} \left[\left(\frac{|\tau|}{\pi\lambda} \right)^{1/2} e^{-x^2/(4\lambda|\tau|)} + \frac{|x|}{2\lambda} \text{erf}\left(\frac{|x|}{\sqrt{4\lambda|\tau|}}\right) \right] \end{aligned} \quad (19a)$$

$$\approx \frac{1}{B} \begin{cases} (|\tau|/\pi\lambda)^{1/2}, & x \ll \sqrt{\lambda|\tau|}, \\ |x|/2\lambda, & x \gg \sqrt{\lambda|\tau|}, \end{cases} \quad (19b)$$

where $\text{erf}(x)$ is the error function. Given these divergent critical ground state fluctuations, it is important to examine the effect of nonlinearities in the action (15). We turn to this next.

C. Perturbation theory and Ginzburg criterion

To this end, it is helpful to first assess the role of nonlinearities

$$S_{\text{nonlinear}} = \int d^d x d\tau \left[-\frac{1}{2} i B_3 (\partial_\tau \theta) (\nabla \theta)^2 + \frac{1}{8} B_4 (\nabla \theta)^4 \right], \quad (20)$$

using a conventional perturbation theory. This can be done by computing perturbative corrections in $S_{\text{nonlinear}}$ (20) to any physical observable, e.g., the effective action itself. Following a standard field-theoretic analysis, at low energies this can be encoded as corrections to the couplings B and K , with the leading contribution to δB , summarized graphically in Eq. (A2) and given by ($T = 0$)

$$\begin{aligned} \delta B &= \frac{1}{2} B_3^2 \int_{\mathbf{k}, \omega} k^4 G(\mathbf{k}, \omega)^2 \\ &= \frac{1}{2} B_3^2 \int \frac{d^d k}{(2\pi)^d} \int_{-\infty}^{\infty} \frac{d\omega}{2\pi} \frac{k^4}{(Kk^4 + r k^2 + B\omega^2)^2} \end{aligned}$$

$$\begin{aligned} &= \left[\frac{C_d \Gamma[(2-d)/2] \Gamma[(d+1)/2]}{8\pi^{1/2}} \frac{B_3^2}{(BK)^{3/2}} \xi^{2-d} \right] B, \\ &= \left[\frac{1}{8\pi} \frac{B_3^2}{(BK)^{3/2}} \xi \right] B, \quad \text{for } d = 1. \end{aligned} \quad (21)$$

In above, we used $\theta(\mathbf{k}, \omega)$ two-point correlation function, $G(\mathbf{k}, \omega)$ [see Eq. (A1)], and focused on zero temperature ground state quantum fluctuations in $d < 2$, which allowed us to take the UV cutoff, $\Lambda \rightarrow \infty$. The dominant contribution from the long-wavelength, low-energy modes is cutoff by the (Gaussian) correlation length $\xi = \sqrt{K/r}$.

Since this nonlinear contribution grows with ξ , sufficiently close to the critical point the correction δB becomes comparable to its bare microscopic value B . This signals a breakdown of the harmonic theory near the critical point on length scales longer than the Ginzburg scale

$$\xi_G = \begin{cases} \left[\frac{8\pi^{1/2}}{C_d \Gamma[(2-d)/2] \Gamma[(d+1)/2]} \frac{(BK)^{3/2}}{B_3^2} \right]^{1/(2-d)}, & d < 2, \\ \frac{8\pi(BK)^{3/2}}{B_3^2}, & d = 1, \end{cases} \quad (22)$$

defined by the value of ξ at which $|\delta B(\xi_G)| = B$. Equivalently, this also gives the Ginzburg criterion $r_G = K\xi_G^{-2}$, corresponding to a “distance” to the critical point at which critical fluctuations qualitatively modify the predictions of the harmonic analysis at the Gaussian fixed point.

D. RG analysis and ϵ expansion

To describe the critical properties beyond the Ginzburg scale, ξ_G , near the critical point with $|r| < r_G$ —i.e., to make sense of the IR divergent perturbation theory found in Eq. (21)—requires a renormalization group analysis. As we discuss in Sec. IV this was first done at the critical dimension of $d = 2$ in the context of a smectic-A to smectic-C liquid crystal phase transition in a seminal work by Grinstein and Pelcovits (GP) [20,21].

To this end, we employ the standard momentum-shell RG transformation [29] by separating the field into long and short scale contributions according to $\theta(\mathbf{x}, \tau) = \theta_<(\mathbf{x}, \tau) + \theta_>(\mathbf{x}, \tau)$ and perturbatively in nonlinearities, $S_{\text{nonlinear}}$, integrate out the short-scale (high momenta) fields $\theta_>(\mathbf{x}, \tau)$ that take support inside an infinitesimal cylindrical momentum-frequency shell $\Lambda e^{-\delta\ell} < k_> < \Lambda \equiv 1/a$, $-\infty < \omega < \infty$. Purely for convenience, we follow this with a rescaling of lengths, times, and the long wavelength part of the field in real space:

$$\mathbf{x} = e^{\delta\ell} \mathbf{x}', \quad \tau = e^{z\delta\ell} \tau', \quad \theta_<(\mathbf{x}, \tau) = e^{\chi\delta\ell} \theta'(\mathbf{x}', \tau'), \quad (23)$$

so as to restore the UV cutoff $e^{-\delta\ell} \Lambda$ back to $\Lambda = 1/a$. Above, z is a dynamical exponent, χ is a field dimension, and ℓ is “RG time.”

The above rescaling leads to zeroth-order RG flows of the effective couplings after coarse-graining by a factor e^ℓ

$$\begin{aligned} r(\ell) &= e^{(d+z-2+2\chi)\ell} r, \\ K(\ell) &= e^{(d+z-4+2\chi)\ell} K, \\ B(\ell) &= e^{(d-z+2\chi)\ell} B, \\ B_3(\ell) &= e^{(d-2+3\chi)\ell} B_3, \\ B_4(\ell) &= e^{(d+z-4+4\chi)\ell} B_4. \end{aligned} \quad (24)$$

To assess the importance of nonlinearities relative to harmonic terms, it is convenient (but not necessary) to keep the quadratic terms fixed under the RG flow, i.e., to choose $K(\ell) = K$ and $B(\ell) = B$, corresponding to a choice of $z = 2$, $\chi = (2-d)/2$. With this, we find $B_3(\ell) = e^{\frac{1}{2}(2-d)\ell} B_3$, $B_4(\ell) = e^{(2-d)\ell} B_4$, reflecting their importance at the critical point $r = 0$, below the upper-critical dimension $d_c = 2$. This is consistent with our finding in Eq. (21) of a divergent perturbation theory for $d < 2$. Since the nonlinearities are irrelevant for $d > d_c$, and thus are only weakly relevant just below $d = 2$, we expect to control our perturbative RG analysis for $d < 2$ by an ε expansion in $\varepsilon = 2 - d$. As discovered by Wilson and Fisher in the context of classical ferromagnet [41], this gives us a controlled method to analyze the critical properties of a physical $d = 1$ ferromagnetic wire, by extrapolating via $\varepsilon = 1$.

The leading one-loop order RG comes from integrating out the high-momentum modes, $\theta_{>}(\mathbf{x}, \tau)$, perturbatively in $S_{\text{nonlinear}}$. The contributions are of the same form as in a direct perturbation theory [e.g., δB in (Sec. III A)], but with the correction kept small by the infinitesimal momentum shell $\delta\ell$. Relegating the technical details to Appendix A, the result of this coarse-graining RG procedure is encoded in ℓ dependent couplings, that we find to satisfy the flow equations (we focus on the $T = 0$ case):

$$\begin{aligned} \frac{dB}{d\ell} &= (d - z + 2\chi)B + \frac{B_3^2 \gamma_d}{B^{1/2}(K + \tilde{r})^{3/2}}, \\ \frac{dB_3}{d\ell} &= (d - 2 + 3\chi)B_3 - \frac{B_3 \gamma_d}{B^{3/2}(K + \tilde{r})^{3/2} d} \\ &\quad \times [(d + 2)BB_4 + 2B_3^2], \\ \frac{dB_4}{d\ell} &= (d - 4 + z + 4\chi)B_4 - \frac{\gamma_d}{B^{5/2}(K + \tilde{r})^{3/2}(d^2 + 2d)} \\ &\quad \times [(d^2 + 6d + 20)B^2 B_4^2 + 4(d + 8)BB_4 B_3^2 + 12B_3^4], \\ \frac{dK}{d\ell} &= (d - 4 + z + 2\chi)K - \frac{B_3^2 \gamma_d}{2B^{3/2}(K + \tilde{r})^{5/2} d(d + 2)} \\ &\quad \times [(2K + \tilde{r})(K + \tilde{r})(d + 2) - 3\tilde{r}^2], \\ \frac{d\tilde{r}}{d\ell} &= (d - 2 + z + 2\chi)\tilde{r} + \frac{2\gamma_d}{B^{3/2}(K + \tilde{r})^{1/2}} \\ &\quad \times (BB_4 + B_3^2)(1 + 2/d), \end{aligned} \quad (25)$$

where we defined $\gamma_d = C_d \Lambda^{d-2}/8$ and $\tilde{r} \equiv r/\Lambda^2$.

As discussed in detail in Appendix A, we note that coarse graining also generates a term $i\delta\alpha_R \partial_\tau \theta$, that is a correction to the average ground state spin current, that thus flows under RG (much like an order parameter in an ordered state). This operator can be shifted away by redefining the average spin current, corresponding to a shift in θ by $\propto \delta\alpha_R \tau$. From the B_3 operator this then generates a correction to $(\nabla\theta)^2$, i.e., a $\delta\alpha_R$ correction to the critical coupling r , which (along with two other contributions, B_3^2 and B_4 tadpole) has been included in the last equation in Eq. (25). Anticipating the connection of the quantum FM transition with the classical smectic liquid crystal, we note that this procedure is analogous to the RG flow of the smectic ordering wave vector, as discussed in Ref. [21].

To bring out the physical content of the above flow equations and to simplify the mathematical analysis, it is convenient to use (25) to construct a flow of two dimensionless couplings

$$g_1 = \frac{B_3^2}{(BK)^{3/2}} \gamma_d, \quad g_2 = \frac{B_4}{(BK^3)^{1/2}} \gamma_d, \quad (26)$$

where for consistency of the ε expansion d must be evaluated at the upper critical dimension, i.e., $\gamma_d \rightarrow \gamma_2 = 1/16\pi$. These couplings can be shown to satisfy dimensionless RG flow equations

$$\frac{dg_1}{d\ell} = \varepsilon g_1 - g_1 \left(\frac{11g_1}{4} + 4g_2 \right), \quad (27a)$$

$$\frac{dg_2}{d\ell} = \varepsilon g_2 - g_2 \left(\frac{19g_1}{4} + \frac{9g_2}{2} \right) - \frac{3g_1^2}{2}, \quad (27b)$$

which we note are independent of the arbitrary rescaling exponent z and χ (that only acquire physical content if B and K are chosen to be kept fixed under coarse graining). In the above, for consistency of the ε expansion we also evaluated d at d_c , i.e., set $d = 2$ in the quadratic terms on the right hand side, and, focusing on the vicinity of a critical point, set $r = 0$.

In terms of g_1 and g_2 the flow of the harmonic couplings is then given by

$$\begin{aligned} \frac{dB}{d\ell} &= [d - z + 2\chi + g_1]B \\ &= [d - z + 2\chi - \eta_B]B, \\ \frac{dK}{d\ell} &= \left[d - 4 + z + 2\chi - \frac{1}{2}g_1 \right]K \\ &= [d - 4 + z + 2\chi + \eta_K]K, \\ \frac{d\tilde{r}}{d\ell} &= [d - 2 + z + 2\chi - 2(g_1 + g_2)]\tilde{r} + 4(g_1 + g_2)K, \end{aligned} \quad (28)$$

where we implicitly defined the anomalous exponents $\eta_{B,K}$, that flow to universal values at a critical point g_1^*, g_2^* . The last term in the \tilde{r} equation corresponds to the fluctuation-driven downward shift of the critical point \tilde{r}_c . The dynamical exponent z , defined by the relation $\tau_\xi \sim \xi^z$ [see (23)] between the correlation time τ_ξ and correlation length $\xi \sim \tilde{r}^{-\nu}$, and the correlation length exponent $\nu = 1/y_r$ (inverse of the eigenvalue y_r of \tilde{r}) are then determined by

$$\begin{aligned} z &= 2 - \frac{1}{2}(\eta_B + \eta_K) = 2 + \frac{3}{4}g_1^*, \\ \nu &= \left(2 - \frac{3}{2}g_1^* - 2g_2^* \right)^{-1}. \end{aligned} \quad (29)$$

The flow diagrams corresponding to (27) are shown in Figs. 1, 2, and 4. As anticipated based on the perturbative analysis and power counting, for $d < 2$, in the presence of quantum fluctuations the Gaussian (G) critical point is unstable to interactions. Simple analysis shows that there are three non-Gaussian critical points: (i) inversion-symmetric (IS) with $g_1 = 0, g_2 > 0$, (ii) smectic (Sm) with $g_1 < 0, g_2 = |g_1|$, (iii) smectic-A to C transition (SmAC) with $g_1 < 0, g_2 \neq |g_1|$, summarized in Table I. We next study the physical significance

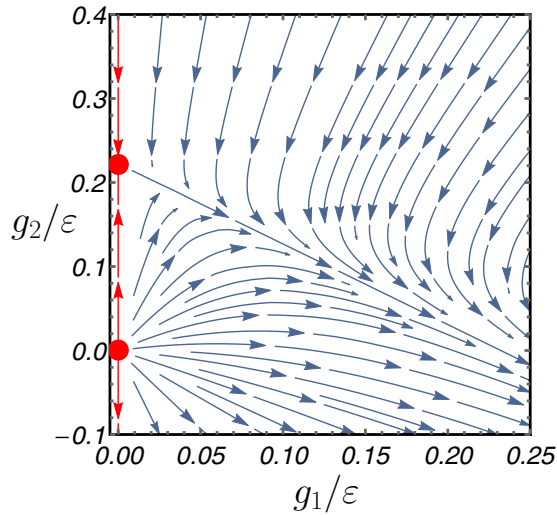


FIG. 1. RG flow of the parameters g_1 and g_2 defined in Eq. (26) describing the FM transition. The flow is given by Eq. (27). Two unstable fixed points are located at the line $g_1 = 0$, see Table I. We see that, at large enough RG time ℓ , g_2 flows to negative values, thus necessarily resulting in a first-order transition.

of these critical points and their critical properties, noting that $g_1 > 0$ and $g_1 < 0$, respectively, are realizable in a FM wire (studied next) and the SmA-C liquid crystal (studied in Sec. IV). We emphasize that all (non-Gaussian) fixed points find realization in certain physical systems, see Secs. III E 1 and IV.

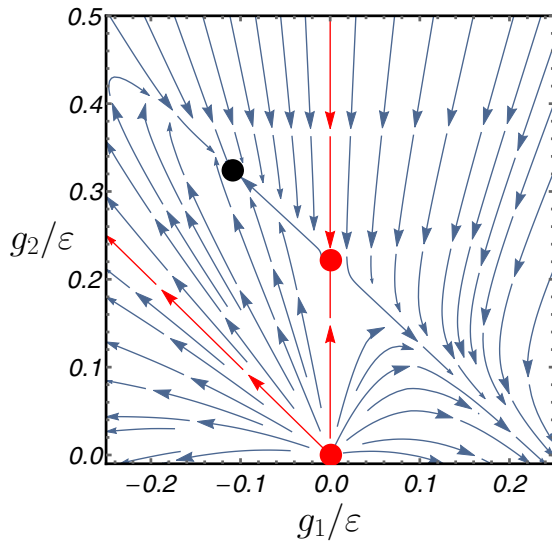


FIG. 2. Global phase diagram of the RG flow described by Eq. (27) for both the FM and SmA-C transitions. The region $g_1 > 0$ describes a runaway flow signaling a first-order phase transition. The line $g_1 = 0$ governs the FM transition in the inversion-symmetric system, which is controlled by the IS fixed point. The region $0 < -g_1 < g_2$ is controlled by an interacting fixed point (black) and describes the second-order SmA-C transition in a magnetic field. The line $-g_1 = g_2$ describes the SmA ‘critical phase,’ with the parameters g_1, g_2 flowing to the Sm fixed point (not shown in this figure, see also Fig. 4).

E. Ferromagnetic transition

It is clear from our derivation of the ferromagnetic model, Eq. (15), and the definition of g_1 , Eq. (26), that for a FM wire the case of physical interest is $g_1 \geq 0$; the other half plane, $g_1 < 0$, does not appear to be accessible to the FM system. However, as we discuss in Sec. IV, it does find a physical realization in smectic liquid crystals.

1. Inversion-symmetric FM

The inversion-symmetric FM is constrained by $B_3 = g_1 = 0$. In this subspace, the flow for g_2 reduces to [see Eqs. (27) and (28)]

$$\frac{dg_2}{d\ell} = \varepsilon g_2 - \frac{9}{2} g_2^2, \quad (30)$$

giving the nontrivial IS critical point,

$$g_1^* = 0, \quad g_2^* = \frac{2\varepsilon}{9}, \quad r^* = -\frac{4\varepsilon\Lambda^2}{9}, \quad (31)$$

previously studied by Kun Yang [15]. This fixed point controls an inversion-symmetric, itinerant PM-to-FM quantum phase transition, and to one-loop order is characterized by

$$\begin{aligned} \eta_B = \eta_K = 0, \quad z = 2, \\ \nu = \frac{1}{2 - 4\varepsilon/9} \approx \frac{1}{2} \left(1 + \frac{2\varepsilon}{9} \right) \approx \frac{11}{18}, \end{aligned} \quad (32)$$

where the last expression for the correlation length exponent ν was evaluated for the physical case of one-dimensional FM wire, $d = 1$ ($\varepsilon = 1$). The other critical exponents, up to linear order in ε , are given by

$$\begin{aligned} \eta = 4 - d - z - 2\chi \approx 0, \\ \gamma = (2 - \eta)\nu \approx \left(1 + \frac{2\varepsilon}{9} \right) \approx \frac{11}{9}, \end{aligned} \quad (33)$$

$$\beta = \frac{\nu}{2}(d + z + \eta - 2) \approx \frac{1}{2} \left(1 - \frac{5\varepsilon}{18} \right) \approx \frac{13}{36},$$

where η is an anomalous dimension, γ is susceptibility exponent, and β is magnetization exponent [42].

2. Inversion-asymmetric FM

We now turn to the main focus of the paper, namely the FM phase transition in an inversion-asymmetric itinerant ferromagnet, with $B_3 \neq 0$. Our key observation is that the inversion-symmetric $g_1 = 0$ fixed point discussed in the previous subsection is unstable to $g_1 \neq 0$, with the symmetry-breaking growth characterized by

$$\frac{dg_1}{d\ell} = \frac{\varepsilon g_1}{9}. \quad (34)$$

It is clear from the RG flows (see Fig. 1), that there is no stable critical point for $g_1 > 0$. Similar fluctuation-driven runaway flows have been discussed in the literature, most prominently in the context of a normal-to-superconductor and (mathematically related) nematic-to-smectic-A phase transitions [43,44]. For small ε , the absence of a stable fixed point was demonstrated via a detailed RG analysis to be a signature of a fluctuation-driven first-order transition [45]. Other examples include crystal-symmetry breaking fields in $O(N)$ magnets [46] and isotropic-to-tetrahedral phase transition [47].

Generically, to demonstrate a fluctuation-driven first-order transition requires a detailed RG computation of the free energy [46]. Here, instead we argue that the inversion-asymmetric itinerant PM-FM phase transition is driven first-order based on qualitative arguments, leaving a detailed computation of the free energy to future studies.

To this end we first observe (see Fig. 1) that for a given bare $B_4 > 0$ and nonzero B_3 , sufficiently close to the $g_1 = 0$ critical point, quantum fluctuations with $g_1 > 0$ always drive B_4 negative. RG analysis allows us to map a nearly critical strongly fluctuating system at small r to a coarse-grained noncritical system at large $r(\ell_*) \sim \Lambda^2$. Then, to find a transition, we can simply minimize the *coarse-grained* Hamiltonian density that approximates the ground-state energy density $\mathcal{E}_{gs}(\tilde{J}, S, r)$

$$\mathcal{E}_{gs} = \frac{1}{2B} \tilde{J}^2 - \frac{B_3}{2B} \tilde{J} S^2 + \frac{r}{2} S^2 + \left(-\frac{|B_4|}{8} + \frac{B_3^2}{8B} \right) S^4 + B_6 S^6, \quad (35)$$

over \tilde{J} and S , where \tilde{J} is proportional to the fluctuations of the spin current about its average value and S is proportional to magnetization. Minimizing over \tilde{J} gives a standard quartic form with the renormalized B_4 driven negative and B_6 included for the overall stability

$$\mathcal{E}_{gs} = \frac{r(\ell_*)}{2} S^2 - \frac{|B_4(\ell_*)|}{8} S^4 + B_6(\ell_*) S^6. \quad (36)$$

We emphasize that all couplings $r(\ell_*)$, $B_3(\ell_*)$, $B_4(\ell_*)$, $B_6(\ell_*)$ in Eqs. (35) and (36) are solutions to the RG flow equations (25) evaluated at ℓ_* defined by $r(\ell_*) \sim \Lambda^2$, or, equivalently, $\ell_*(r_*) = \ln[\xi(r_*)/a]$.

Because the mapped system lies outside the Ginzburg region, where fluctuations are small, its ground state energy and the associated transition can be computed within mean-field approximation. We thus find that a weakly first-order transition takes place at r_* , with a magnetization jump S_* implicitly determined by

$$r_* \approx \frac{B_4^2(\ell_*)}{128 B_6(\ell_*) e^{2\ell_*}}, \quad (37a)$$

$$S_* \approx \left(\frac{8r_*}{|B_4(\ell_*)|} \right)^{1/2}. \quad (37b)$$

To summarize, we find a strong, general result, that the itinerant PM-FM transition in the absence of inversion symmetry *must be first order*. This contrasts qualitatively from the inversion-symmetric case and the Hertz-Millis expectation of a continuous transition.

IV. SMECTIC-A-C TRANSITION IN A MAGNETIC FIELD

As we discuss in detail below, quite remarkably the model of the itinerant PM-FM quantum phase transition studied above is mathematically equivalent to that of a classical D -dimensional smectic-A to smectic-C liquid crystal transition in a magnetic field [37,38]. We recall that a smectic-A liquid crystal is a one-dimension density wave (a one-dimensional periodic array of 2D liquid sheets) of rodlike constituents (calamitic molecules) defined by director \hat{n} aligned along the smectic layer normal, \hat{k} , spontaneously breaking rotational

and one-dimensional translational symmetries. To match the notation of the FM action (15), we denote the latter spatial axis (conventionally denoted by z) to be τ , with the smectic classical Hamiltonian given by

$$H_{\text{SmA}} = \int d^2x d\tau \left[\frac{K}{2} (\nabla_{\perp}^2 u)^2 + \frac{B}{2} \left(\partial_{\tau} u - \frac{1}{2} (\nabla_{\perp} u)^2 \right)^2 \right], \quad (38)$$

where u is the smectic scalar phonon field that describes distortions of smectic layers along the layer normal. We note that the underlying rotational invariance of the smectic phase is encoded through the nonlinearities appearing only via a fully rotationally invariant strain, $u_{\tau\tau} = \partial_{\tau} u - \frac{1}{2} (\nabla_{\perp} u)^2$, that at harmonic level reduces to the absence of the quadratic $(\nabla_{\perp} u)^2$ term in Eq. (38). The latter would otherwise incorrectly penalize a rotation of the smectic layers by an infinitesimal angle $\theta \approx \nabla_{\perp} u$ [21,38].

As illustrated in Fig. 3, a smectic-C liquid crystal is distinguished by a spontaneous molecular tilt of \hat{n} into the smectic planes, i.e., $\hat{n} \cdot \hat{k} < 1$. The associated XY order parameter is the \vec{c} director, a projection of \hat{n} into the smectic planes, characterized by an effective Hamiltonian (within a single elastic constant K approximation)

$$H_c = \int d^2x d\tau \left[\frac{K}{2} (\nabla_{\perp} \vec{c})^2 + \frac{r}{2} c^2 + \frac{\lambda}{4} c^4 \right], \quad (39)$$

with the reduced temperature $r \sim T - T_{AC}$ driving the AC transition.

A model for smectic A-C transition was proposed by Chen and Lubensky [48], and then extensively studied by Grinstein and Pelcovits [20], who demonstrated that, despite the nontrivial coupling of the \vec{c} -director XY model (39) to the smectic phonon u elasticity (38), the criticality remains of a conventional XY -model (superfluid Helium-4 transition) universality class, as originally conjectured by de Gennes [37].

In a magnetic field \vec{h} , the liquid crystal molecules with positive diamagnetic anisotropy align along the field, with the energetics governed by

$$H_{\text{field}} = -\frac{1}{2} \chi_a \int d^2x d\tau (\hat{n} \cdot \vec{h})^2, \quad (40a)$$

$$\approx -\frac{h^2}{2} \chi_a \int d^2x d\tau [1 - (\vec{c} - \nabla_{\perp} u)^2] \quad (40b)$$

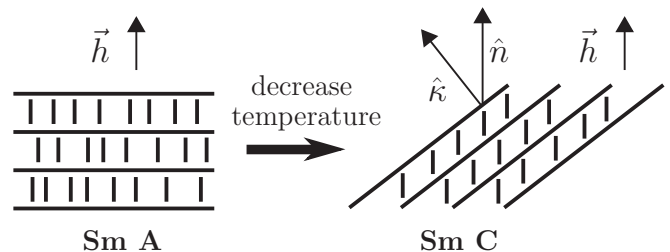


FIG. 3. Schematic representation of the smectic-A to smectic-C transition in a magnetic field, \vec{h} . The transition occurs via tilting of the layers, and is characterized by a nonzero angle between the molecules' director \hat{n} and the smectic layer normal, \hat{k} (see Ref. [20]).

TABLE I. The fixed points of the one-loop RG flow (27) describing the FM and SmA-C transitions. In the corresponding regions of stability, critical points are characterized by an anomalous dimension η , correlation length critical exponent ν , susceptibility exponent γ , and order parameter exponent β .

Fixed point	g_1	g_2	η_B	η_K	r	z	χ	ν	γ	β	stability
G	0	0	0	0	0	2	$\varepsilon/2$	1/2	1	1/2	unstable
IS	0	$2\varepsilon/9$	0	0	$-4\varepsilon/9$	2	$\varepsilon/2$	$(9+2\varepsilon)/18$	$1+(2\varepsilon/9)$	$(18-5\varepsilon)/36$	unstable
Sm	$-4\varepsilon/5$	$4\varepsilon/5$	$4\varepsilon/5$	$2\varepsilon/5$	0	$2-(3\varepsilon/5)$	$3\varepsilon/5$	—	—	—	unstable
SmAC	$-4\varepsilon/37$	$12\varepsilon/37$	$4\varepsilon/37$	$2\varepsilon/37$	$-16\varepsilon/37$	$2-(3\varepsilon/37)$	$19\varepsilon/37$	$(37+9\varepsilon)/74$	$1+(\varepsilon/74)$	$(37-10\varepsilon)/74$	stable

with χ_a the associated susceptibility. As was discussed by GP and illustrated in Fig. 3, because the molecules are locked along the field \vec{h} , the AC transition in a magnetic field is associated with the spontaneous tilt of smectic layers toward the magnetic field axis.

Furthermore, because the underlying rotational symmetry is broken by the \vec{h} field, the nature of transition is qualitatively modified. Indeed, neither Sm-A nor Sm-C is any longer rotationally invariant. It is clear that the magnetic field locks the \vec{c} director to layer tilt, $\vec{c} \approx \nabla_{\perp} u$, allowing one to reexpress $H_c[\vec{c} \rightarrow \nabla_{\perp} u]$ in terms of u , formally done by integrating out the \vec{c} director. Not surprisingly, this leads to a smecticlike Hamiltonian, but with the rotational symmetry broken by the magnetic field \vec{h} , and the smectic A-C transition described by a classical Hamiltonian [20]

$$H_{\text{SmACfield}} = \int d^{D-1} x d\tau \left[\frac{K}{2} (\nabla_{\perp}^2 u)^2 + \frac{r}{2} (\nabla_{\perp} u)^2 + \frac{B}{2} (\partial_{\tau} u)^2 - \frac{B_3}{2} (\partial_{\tau} u) (\nabla_{\perp} u)^2 + \frac{B_4}{8} (\nabla_{\perp} u)^4 \right], \quad (41)$$

generalized to $D = d + 1$ dimensions. Clearly, at the Sm critical point, which is characterized by $r = 0$ and by a special relation of the nonlinearities, $B_3 = B_4 = B$, this reduces to the fully rotationally invariant smectic elasticity, Eq. (38).

We next note that this classical Hamiltonian for the smectic A-C transition is identical in form to that of the itinerant quantum PM-FM transition (15), studied in the previous section. However, a key difference is the absence of i in the B_3 term of the classical problem. Thus, the smectic A-C transition maps directly onto our FM transition analysis in Sec. III, but with the dimensionless coupling $g_1 \sim -B_3^2 < 0$. It thus allows us to access the $g_1 < 0$ half of the flow diagram in Fig. 2, and in particular the two additional critical points, that with some foresight we earlier denoted by Sm and SmAC (see also Table I and Fig. 4).

The most ubiquitous case of a three-dimensional smectic lies right at the upper critical dimension, $D = D_{cr} = 3$ ($d = 2$), and has been extensively analyzed in Refs. [20,21]. Our results, summarized by equations (27) and (28) are a generalization of GP's work to arbitrary dimension and in particular to $D < 3$, where the nonlinearities are relevant (rather than marginally irrelevant [20,21]) and lead to nontrivial fixed points, illustrated in Fig. 4.

As is clear from the RG flows, the Gaussian and IS critical points, discussed in the context of the FM transition, are unstable to the Sm and SmAC fixed points. The SmAC critical point is the one with global stability (to order ε) and thus controls the smectics-A to smectic-C phase transition in a

magnetic field. It is given by

$$g_2^* = -3g_1^* = \frac{12\varepsilon}{37}, \quad r^* = -\frac{16\varepsilon}{37}, \quad (42)$$

and is characterized by the anomalous universal exponents

$$\begin{aligned} \eta_B &= 2\eta_K = \frac{4\varepsilon}{37} \approx \frac{4}{37}, \\ z &\approx 2 - \frac{3\varepsilon}{37} \approx \frac{71}{37}, \\ \eta &\approx \frac{17\varepsilon}{37} \approx \frac{17}{37}, \\ \nu &\approx \frac{1}{2} \left(1 + \frac{9\varepsilon}{37} \right) \approx \frac{23}{37}, \\ \gamma &\approx 1 + \frac{\varepsilon}{74} \approx \frac{75}{74}, \\ \beta &\approx \frac{1}{2} \left(1 - \frac{10\varepsilon}{37} \right) \approx \frac{27}{74}, \end{aligned} \quad (43)$$

evaluated for the only case of physical interest, the two-dimensional smectic $D = 2$ ($\varepsilon = 1$).

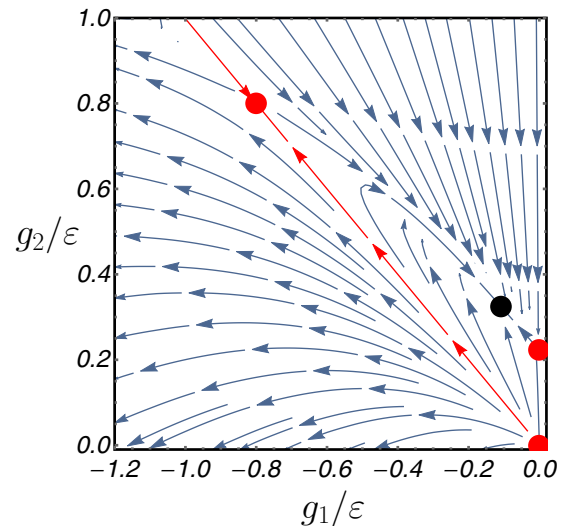


FIG. 4. The RG flow for the SmA-C transition in a magnetic field described by Eq. (27) in the region $g_1 < 0$ ($g_1 < 0$ part of Fig. 2). A stable fixed point (black) controls the second-order transition. The region $g_2 < |g_1|$ corresponds to the mechanical instability of the system, and, thus, describes a first-order transition. The separatrix $|g_1| = g_2$, which separates two regions (red line), corresponds to the SmA line, and is controlled by the Sm fixed point.

From the global phase diagram perspective (see Fig. 2), we thus find that the phase transition is continuous for $g_1 < 0$ (controlled by the SmAC critical point in the region of mechanical stability, $g_2 > |g_1|$); in the region $g_2 < |g_1|$, higher-order terms are needed to stabilize a theory, and a transition is automatically first order) and is driven by fluctuations to be first order for $g_1 > 0$. The two regimes are then separated by the inversion-symmetric tricritical IS point at $g_1 = 0$.

The other critical point is the unstable Sm fixed point, characterized by $-g_1 = g_2 > 0$ or, equivalently, $B_3^2 = B_2 B_4$. We note that in this coupling subspace, the nonlinearities assemble into a complete square of a nonlinear strain tensor

$$\begin{aligned} & \frac{B}{2}(\partial_\tau u)^2 - \frac{B_3}{2}(\partial_\tau u)(\nabla_\perp u)^2 + \frac{B_4}{8}(\nabla_\perp u)^4 \\ &= \frac{B}{2} \left[\partial_\tau u - \frac{1}{2} \sqrt{\frac{B_4}{B}} (\nabla_\perp u)^2 \right]^2, \end{aligned} \quad (44)$$

that after an inconsequential rescaling of the phonon u reduces to a fully rotationally invariant nonlinear smectic elasticity, Eq. (38). We note that from Eq. (27) we find that $\bar{g} = g_1 + g_2$ flows according to

$$\frac{d\bar{g}}{d\ell} = \varepsilon \bar{g} - \frac{\bar{g}}{4} (17g_1 + 18g_2), \quad (45)$$

ensuring that the smectic line $\bar{g} = 0$ (defined by full nonlinear rotational invariance, $g_1 = -g_2$) is preserved. Examining Eqs. (27) and (28) we further note that this Sm fixed point is stable inside the $-g_1 = g_2 \equiv g, r = 0$ subspace (the flow of r reduces to a homogeneous equation), with the flow reducing to that of a single coupling g

$$\frac{dg}{d\ell} = \varepsilon g - \frac{5}{4} g^2, \quad (46)$$

and harmonic couplings

$$\frac{dB(\ell)}{d\ell} = (D - 1 - z + 2\chi - g(\ell))B(\ell), \quad (47a)$$

$$\frac{dK(\ell)}{d\ell} = \left(D - 5 + z + 2\chi + \frac{1}{2}g(\ell) \right) K(\ell). \quad (47b)$$

The Sm fixed point, previously studied in Refs. [23,49], is given by $g^* = 4\varepsilon/5$, $\chi = 3\varepsilon/5$, $\eta_B = 4\varepsilon/5$, $\eta_K = 2\varepsilon/5$, and $z = 2 - 3\varepsilon/5$. As its name implies, it actually describes strongly-fluctuating finite T properties of a D -dimensional smectic-A, which is thus an example of a ‘‘critical phase’’ [49].

This Sm fixed point is an ε -expansion approximation for a two-dimensional smectic. As was shown by Golubovic and Wang [22,23], remarkably, the universal exponents of a $D = 2$ smectic can be obtained *exactly* through its mapping onto nonequilibrium dynamics of a 1+1-dimensional Kardar-Parisi-Zhang (KPZ) equation [24]. The exponents for the latter were deduced to be $\chi = 1/2$, $z = 3/2$, *exactly* [50]. Curiously, an uncontrolled one-loop approximation done directly in $D = 2$ smectic also gives these exponents exactly [23].

We utilize RG flows (46) and (47) to compute the long-scale smectic phonon correlation function, finding

$$C(\mathbf{k}_\perp, k_\tau) \approx \frac{T}{B(\mathbf{k})k_\tau^2 + K(\mathbf{k})k_\perp^4}, \quad (48)$$

with moduli $B(\mathbf{k})$ and $K(\mathbf{k})$ that are singularly wave-vector-dependent. These moduli are determined by the solutions $B(\ell)$ and $K(\ell)$ of the RG flow equations (47a) and (47b), with the initial conditions set by the microscopic values of B and K .

In $D = 2$ (implying $\varepsilon = 1$), the scale at which the nonlinearities become important is given by $\xi_\perp^{NL} = \frac{1}{T} \left(\frac{K^3}{B} \right)^{1/2}$ [49]. At scales longer than ξ_\perp^{NL} , the nonlinear coupling $g(\ell)$ flows to the Sm fixed point $g^* = 4/5$, and the RG matching analysis predicts anisotropic wave-vector-dependent moduli

$$\begin{aligned} K(\mathbf{k}) &= K(k_\perp \xi_\perp^{NL})^{-\eta_K} f_K(k_\tau \xi_\tau^{NL} / (k_\perp \xi_\perp^{NL})^z), \\ &\sim k_\perp^{-\eta_K}, \end{aligned} \quad (49a)$$

$$\begin{aligned} B(\mathbf{k}) &= B(k_\perp \xi_\perp^{NL})^{\eta_B} f_B(k_\tau \xi_\tau^{NL} / (k_\perp \xi_\perp^{NL})^z), \\ &\sim k_\perp^{\eta_B}, \end{aligned} \quad (49b)$$

with universal scaling functions, $f_B(x)$, $f_K(x)$ that we will not compute here. The anomalous exponents in $D = 2$ ($\varepsilon = 1$) are given by

$$\eta_B = g^* = \frac{4}{5}, \quad (50a)$$

$$\eta_K = \frac{1}{2}g^* = \frac{2}{5}, \quad (50b)$$

$$z = 2 - \frac{1}{2}(\eta_B + \eta_K) = \frac{7}{5}. \quad (50c)$$

The underlying rotational invariance of the Sm fixed point gives an *exact* relation between the two anomalous $\eta_{B,K}$ exponents

$$3 - D = \frac{\eta_B}{2} + \frac{3}{2}\eta_K, \quad (51a)$$

$$1 = \frac{\eta_B}{2} + \frac{3}{2}\eta_K, \quad \text{for } D = 2, \quad (51b)$$

which is obviously satisfied by the anomalous exponents, Eqs. (50a) and (50b), computed here to first order in $\varepsilon = 3 - D$. In $D = 3$, this analysis reduces to the exact logarithmically renormalized $B(\mathbf{k})$ and $K(\mathbf{k})$ found by Grinstein and Pelcovits [20].

V. SUMMARY AND CONCLUSIONS

To summarize, we studied the quantum Ising ferromagnetic transition in a one-dimensional system of itinerant electrons. Starting with a microscopic model of a quantum wire with Rashba spin-orbit coupling, we derived a bosonized effective low-energy theory that governs the transition. To analyze the theory, we used a renormalization group approach, controlled by an ε expansion. We showed that in the general case, when inversion symmetry is absent, strong spin fluctuations necessarily drive the transition *first order*, in contrast to the inversion-symmetric case and the predictions of Hertz-Millis theory.

While in the present paper we consider a 1d bosonized model, we conjecture that the first-order transition is a qualitative property that extends to two- and three-dimensional itinerant ferromagnets without inversion symmetry. This conjecture serves as a motivation for future study of the nature of quantum ferromagnetic transition in higher dimensions.

As a byproduct of our analysis, we demonstrated that the imaginary time $D = 1 + 1$ action of the ferromagnetic wire

can be mapped onto the problem of a two-dimensional smectic-A to smectic-C transition in a magnetic field. The range of parameters in the latter problem, however, is inaccessible for the problem of a ferromagnetic transition, and thus leads to qualitatively different physics. In particular, we showed that the Sm-A to Sm-C transition in two dimensions is *second order*, controlled by a newly found stable critical point.

Finally, we constructed the global phase diagram for a bosonic field theory that describes both ferromagnetic and Sm-A to Sm-C phase transitions. We demonstrated that a region of the first-order transition, $g_1 > 0$, is separated from the continuous transition, $0 < -g_1 < g_2$, by a tricritical point at $g_1 = 0$, which describes the FM transition in the presence of inversion symmetry.

ACKNOWLEDGMENTS

L.R. thanks John Toner for discussions and for letting us know that he independently derived the RG equations for the SmA-to-SmC transition in a magnetic field in unpublished work. This project was funded by the DOE Office of Basic Energy Sciences, Division of Materials Sciences and Engineering under award DE-SC0010526 (V.K. and L.F.). J.R. acknowledges a fellowship from the Gordon and Betty Moore Foundation under the EPiQS initiative (Grant No.

GBMF4303). L.R. was supported by the Simons Investigator award from the Simons Foundation, by the NSF under Grant No. DMR-1001240C, and by the KITP under Grant No. NSF PHY-1125915. L.R. thanks the KITP for its hospitality as part of the Synthetic Matter workshop and sabbatical program, when part of this work was completed.

APPENDIX: DERIVATION OF RG EQUATIONS


In this Appendix we demonstrate the derivation of RG equations (25). We focus on the FM transition which is described by the effective action (15). To obtain the description of Sm phases, it is sufficient to substitute $B_3 \rightarrow iB_3$.

To calculate the one-loop corrections to the RG equations, we start with a bare Green's function $G_0(\omega, \mathbf{k})$,

$$G_0(\omega, \mathbf{k}) = \frac{1}{B\omega^2 + rk^2 + Kk^4}, \tag{A1}$$

and treat the nonlinear terms, B_3 and B_4 , as a small perturbation. Next, integrating out high momenta modes in the shell $\Lambda e^{-\delta\ell} < k < \Lambda$, $-\infty < \omega < \infty$, we obtain corrections to the parameters of the effective action (15), see Sec. III for details. The one-loop calculation is somewhat tedious but straightforward.

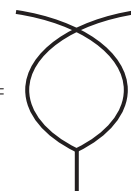
The correction to B is given by a single diagram:



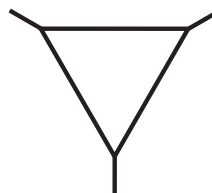
$$\begin{aligned} \delta B &= \text{Diagram} = \frac{B_3^2}{2} \int_{-\infty}^{\infty} \frac{d\omega}{2\pi} \int_{\Lambda e^{-\delta\ell}}^{\Lambda} \frac{d^d k}{(2\pi)^d} \frac{k^4}{(B\omega^2 + rk^2 + Kk^4)^2} \\ &= \frac{B_3^2}{2} \int_{>} \frac{d\omega d^d k}{(2\pi)^{d+1}} \frac{k^4}{(B\omega^2 + rk^2 + Kk^4)^2} = \frac{B_3^2}{B^{1/2}(K + \tilde{r})^{3/2}} \gamma_d \delta\ell, \end{aligned} \tag{A2}$$

where we defined $\tilde{r} \equiv r/\Lambda^2$, $\gamma_d \equiv S_d \Lambda^{d-2}/8(2\pi)^d$, and S_d is the area of the sphere of unit radius in d dimensions. For integer dimensions, it is given by $S_1 = 2$, $S_2 = 2\pi$, $S_3 = 4\pi$ etc. We also use a short notation $\int_{>} d\omega d^d k \dots \equiv \int_{-\infty}^{\infty} d\omega \int_{\Lambda e^{-\delta\ell}}^{\Lambda} d^d k \dots$ for a momentum shell integration hereafter.

The correction to B_3 is given by two diagrams:



$$\delta B_3^{(1)} = \text{Diagram} = -\frac{B_3 B_4}{2} \left(1 + \frac{2}{d}\right) \int_{>} \frac{d\omega d^d k}{(2\pi)^{d+1}} \frac{k^4}{(B\omega^2 + rk^2 + Kk^4)^2} = -\left(1 + \frac{2}{d}\right) \frac{B_3 B_4}{B^{1/2}(K + \tilde{r})^{3/2}} \gamma_d \delta\ell, \tag{A3}$$



$$\delta B_3^{(2)} = \text{Diagram} = -\frac{4}{d} B_3^3 \int_{>} \frac{d\omega d^d k}{(2\pi)^{d+1}} \frac{\omega^2 k^4}{(B\omega^2 + rk^2 + Kk^4)^3} = -\frac{2}{d} \frac{B_3^3}{B^{3/2}(K + \tilde{r})^{3/2}} \gamma_d \delta\ell. \tag{A4}$$

Summing them up, we find

$$\delta B_3 = \delta B_3^{(1)} + \delta B_3^{(2)} = -\frac{B_3 \gamma_d \delta\ell}{B^{3/2}(K + \tilde{r})^{3/2} d} [(d + 2)B_2 B_4 + 2B_3^2]. \tag{A5}$$

The correction to B_4 is given by three diagrams:

$$\delta B_4^{(1)} = \text{Diagram 1} = -\frac{d^2 + 6d + 20}{2d(d+2)} B_4^2 \int_{>} \frac{d\omega d^d k}{(2\pi)^{d+1}} \frac{k^4}{(B\omega^2 + rk^2 + Kk^4)^2} = -\frac{d^2 + 6d + 20}{d(d+2)} \frac{B_4^2}{B^{1/2}(K + \tilde{r})^{3/2}} \gamma_d \delta\ell, \quad (\text{A6})$$

$$\delta B_4^{(2)} = \text{Diagram 2} = -8 \frac{d+8}{d(d+2)} B_3^2 B_4 \int_{>} \frac{d\omega d^d k}{(2\pi)^{d+1}} \frac{\omega^2 k^4}{(B\omega^2 + rk^2 + Kk^4)^3} = -4 \frac{d+8}{d(d+2)} \frac{B_3^2 B_4}{B^{3/2}(K + \tilde{r})^{3/2}} \gamma_d \delta\ell, \quad (\text{A7})$$

$$\delta B_4^{(3)} = \text{Diagram 3} = -\frac{48}{d(d+2)} B_3^4 \int_{>} \frac{d\omega d^d k}{(2\pi)^{d+1}} \frac{\omega^4 k^4}{(B\omega^2 + rk^2 + Kk^4)^4} = -\frac{12}{d(d+2)} \frac{B_3^4}{B^{5/2}(K + \tilde{r})^{3/2}} \gamma_d \delta\ell. \quad (\text{A8})$$

After summation, we find

$$\delta B_4 = \delta B_4^{(1)} + \delta B_4^{(2)} + \delta B_4^{(3)} = -\frac{\gamma_d \delta\ell}{B^{5/2}(K + \tilde{r})^{3/2} d(d+2)} [(d^2 + 6d + 20)B^2 B_4^2 + 4(d+8)B B_4 B_3^2 + 12B_3^4]. \quad (\text{A9})$$

The correction to K is obtained from the same diagram as the correction to B . However, now the external legs of the diagram correspond to spatial derivatives of the field θ , $\partial_x^2 \theta$, rather than time derivatives, as in the case of B . Furthermore, since K couples to the square of the *second* derivative, one needs to expand the exact expression for this diagram to the next-to-leading order in slow external momentum. The result reads as

$$\delta K = \text{Diagram 4} = -\frac{B_3^2 \gamma_d \delta\ell}{2B^{3/2}(K + \tilde{r})^{5/2}} \left[\frac{(2K + \tilde{r})(K + \tilde{r})}{d} - \frac{3\tilde{r}^2}{d(d+2)} \right]. \quad (\text{A10})$$

Finally, there are three contributions to the correction to \tilde{r} . Two of them can be calculated directly from the one-loop diagrams:

$$\delta \tilde{r}^{(1)} = \text{Diagram 5} = \frac{1}{2} \left(1 + \frac{2}{d}\right) B_4 \Lambda^{-2} \int_{>} \frac{d\omega d^d k}{(2\pi)^{d+1}} \frac{k^2}{B\omega^2 + rk^2 + Kk^4} = 2 \left(1 + \frac{2}{d}\right) \frac{B_4}{B^{1/2}(K + \tilde{r})^{1/2}} \gamma_d \delta\ell, \quad (\text{A11})$$

$$\delta \tilde{r}^{(2)} = \text{Diagram 6} = \frac{2}{d} B_3^2 \Lambda^{-2} \int_{>} \frac{d\omega d^d k}{(2\pi)^{d+1}} \frac{\omega^2 k^2}{(B\omega^2 + rk^2 + Kk^4)^2} = \frac{4}{d} \frac{B_3^2}{B^{3/2}(K + \tilde{r})^{1/2}} \gamma_d \delta\ell. \quad (\text{A12})$$

To obtain the third contribution, we consider the diagram that generates a new term in the effective action, $i(\delta r_\tau/2)\partial_\tau \theta$:

$$\delta r_\tau = \text{Diagram 7} = -B_3 \int_{>} \frac{d\omega d^d k}{(2\pi)^{d+1}} \frac{k^2}{B\omega^2 + rk^2 + Kk^4} = -4 \frac{B_3 \Lambda^2}{B^{1/2}(K + \tilde{r})^{1/2}} \gamma_d \delta\ell. \quad (\text{A13})$$

This term describes the correction to the average spin current and can be absorbed by shifting $\partial_\tau \theta \rightarrow \partial_\tau \theta - i\delta r_\tau/2B$ (or, equivalently, $\theta \rightarrow \theta - i\tau \delta r_\tau/2B$), such that $\partial_\tau \theta$ always describes *deviation* from the average spin current, i.e., $\langle \partial_\tau \theta \rangle = 0$. This

extra step of RG, however, generates an additional correction to \tilde{r} , which reads as

$$\delta\tilde{r}^{(3)} = -\frac{B_3\delta r_\tau\Lambda^{-2}}{2B} = 2\frac{B_3^2}{B^{3/2}(K+\tilde{r})^{1/2}}\gamma_d\delta\ell. \quad (\text{A14})$$

After summation, we find

$$\delta\tilde{r} = \delta\tilde{r}^{(1)} + \delta\tilde{r}^{(2)} + \delta\tilde{r}^{(3)} = 2\left(1 + \frac{2}{d}\right)\frac{BB_4 + B_3^2}{B^{3/2}(K+\tilde{r})^{1/2}}\gamma_d\delta\ell. \quad (\text{A15})$$

Collecting together Eqs. (A2), (A5), (A9), (A10), and (A15) we exactly obtain the one-loop part of the RG set of equations (25).

-
- [1] J. A. Hertz, *Phys. Rev. B* **14**, 1165 (1976).
 [2] A. J. Millis, *Phys. Rev. B* **48**, 7183 (1993).
 [3] D. Belitz, T. R. Kirkpatrick, M. T. Mercaldo, and S. L. Sessions, *Phys. Rev. B* **63**, 174427 (2001).
 [4] D. Belitz, T. R. Kirkpatrick, M. T. Mercaldo, and S. L. Sessions, *Phys. Rev. B* **63**, 174428 (2001).
 [5] A. Abanov, A. V. Chubukov, and J. Schmalian, *Adv. Phys.* **52**, 119 (2003).
 [6] J. Rech, C. Pépin, and A. V. Chubukov, *Phys. Rev. B* **74**, 195126 (2006).
 [7] D. Belitz and T. R. Kirkpatrick, *Phys. Rev. Lett.* **89**, 247202 (2002).
 [8] T. R. Kirkpatrick and D. Belitz, *Phys. Rev. B* **67**, 024419 (2003).
 [9] A. V. Chubukov, C. Pépin, and J. Rech, *Phys. Rev. Lett.* **92**, 147003 (2004).
 [10] S. S. Lee, *Phys. Rev. B* **80**, 165102 (2009).
 [11] M. A. Metlitski and S. Sachdev, *Phys. Rev. B* **82**, 075127 (2010); **82**, 075128 (2010).
 [12] D. F. Mross, J. McGreevy, H. Liu, and T. Senthil, *Phys. Rev. B* **82**, 045121 (2010).
 [13] A. L. Fitzpatrick, S. Kachru, J. Kaplan, and S. Raghu, *Phys. Rev. B* **88**, 125116 (2013).
 [14] M. Brando, D. Belitz, F. M. Grosche, and T. R. Kirkpatrick, *Rev. Mod. Phys.* **88**, 025006 (2016).
 [15] K. Yang, *Phys. Rev. Lett.* **93**, 066401 (2004).
 [16] K. Sengupta and Y. B. Kim, *Phys. Rev. B* **71**, 174427 (2005).
 [17] E. H. Lieb and D. Mattis, *Phys. Rev.* **125**, 164 (1962).
 [18] S. Daul and R. M. Noack, *Phys. Rev. B* **58**, 2635 (1998).
 [19] D. J. Bergman and B. I. Halperin, *Phys. Rev. B* **13**, 2145 (1976).
 [20] G. Grinstein and R. A. Pelcovits, *Phys. Rev. A* **26**, 2196 (1982).
 [21] G. Grinstein and R. A. Pelcovits, *Phys. Rev. Lett.* **47**, 856 (1981).
 [22] L. Golubović and Z.-G. Wang, *Phys. Rev. Lett.* **69**, 2535 (1992).
 [23] L. Golubović and Z.-G. Wang, *Phys. Rev. E* **49**, 2567 (1994).
 [24] M. Kardar, G. Parisi, and Y.-C. Zhang, *Phys. Rev. Lett.* **56**, 889 (1986).
 [25] J. Ruhman and E. Berg, *Phys. Rev. B* **90**, 235119 (2014).
 [26] V. Mourik, K. Zuo, S. M. Frolov, S. R. Plissard, E. P. A. M. Bakkers, and L. P. Kouwenhoven, *Science* **336**, 1003 (2012).
 [27] A. Das, Y. Ronen, Y. Most, Y. Oreg, M. Heiblum, and H. Shtrikman, *Nat. Phys.* **8**, 887 (2012).
 [28] P. Krogstrup, N. L. B. Ziino, W. Chang, S. M. Albrecht, M. H. Madsen, E. Johnson, J. Nygård, C. M. Marcus, and T. S. Jespersen, *Nat. Mater.* **14**, 400 (2015).
 [29] M. E. Fisher, *Rev. Mod. Phys.* **46**, 597 (1974).
 [30] T. Giamarchi, *Quantum Physics in One Dimension* (Oxford University Press, New York, 2003).
 [31] A. Luther and V. J. Emery, *Phys. Rev. Lett.* **33**, 589 (1974).
 [32] S. Sachdev, *Quantum Phase Transitions* (Cambridge University Press, New York, 2011).
 [33] M. Kardar, *Statistical Physics of Fields* (Cambridge University Press, New York, 2007).
 [34] J. Ruhman, V. Kozii, and L. Fu, *Phys. Rev. Lett.* **118**, 227001 (2017).
 [35] In fact, there are terms which couple charge and spin sectors that are relevant near the Gaussian fixed point. However, after integrating out the charge sector, these terms only contribute operators that are already present in Eq. (15) and thus do not change the analysis for a PM-FM transition [15]. Despite this, a preliminary analysis shows that critical fluctuations in the spin sector feedback to renormalize the charge sector. In particular, we expect that this leads to a nontrivial $z > 1$ (rather than $z = 1$ at the Gaussian fixed point) dynamical exponent for the charge sector.
 [36] S. Teber, *Phys. Rev. B* **76**, 045309 (2007). For more technical details, see also arXiv version of the paper, where more appendices are included: [arXiv:cond-mat/0609754](https://arxiv.org/abs/cond-mat/0609754).
 [37] P. G. de Gennes and J. Prost, *The Physics of Liquid Crystals* (Clarendon Press, Oxford, 1993).
 [38] P. M. Chaikin and T. C. Lubensky, *Principles of Condensed Matter Physics* (Cambridge University Press, Cambridge, 1995).
 [39] A. Caillé, *C. R. Acad. Sci., Ser. B* **274**, 891 (1972).
 [40] J. Toner and D. R. Nelson, *Phys. Rev. B* **23**, 316 (1981).
 [41] K. G. Wilson and M. E. Fisher, *Phys. Rev. Lett.* **28**, 240 (1972).
 [42] Here we corrected numerical values of critical exponents at IS critical point obtained in Ref. [15] online.
 [43] B. I. Halperin, T. C. Lubensky, and S. K. Ma, *Phys. Rev. Lett.* **32**, 292 (1974).
 [44] J.-H. Chen, T. C. Lubensky, and D. R. Nelson, *Phys. Rev. B* **17**, 4274 (1978).
 [45] Using duality to map a superconductor onto an XY model it was shown [51] that, in fact, (fluctuation-driven first-order transition based on $\varepsilon = 4 - d$ -expansion notwithstanding) a 3d normal-to-superconductor phase transition can be continuous. This suggests a change in behavior and appearance of a tricritical point for $\varepsilon \rightarrow 1$.
 [46] J. Rudnick and D. R. Nelson, *Phys. Rev. B* **13**, 2208 (1976).
 [47] L. Radzihovsky and T. C. Lubensky, *Europhys. Lett.* **54**, 206 (2001).
 [48] J.-H. Chen and T. C. Lubensky, *Phys. Rev. A* **14**, 1202 (1976).
 [49] L. Radzihovsky, *Phys. Rev. A* **84**, 023611 (2011).
 [50] D. A. Huse, C. L. Henley, and D. S. Fisher, *Phys. Rev. Lett.* **55**, 2924 (1985).
 [51] C. Dasgupta and B. I. Halperin, *Phys. Rev. Lett.* **47**, 1556 (1981).